ATP specifically drives refolding of non-native conformations of cytochrome *c*

FEDERICA SINIBALDI,[1] GIAMPIERO MEI,[1] FABIO POLTICELLI,[2] M. CRISTINA PIRO,[1] BARRY D. HOWES,[3] GIULIETTA SMULEVICH,[3] ROBERTO SANTUCCI,[1] FRANCA ASCOLI,[1] AND LAURA FIORUCCI[1]

[1]Dipartimento di Medicina Sperimentale e Scienze Biochimiche, Università di Roma "Tor Vergata," 00133 Roma, Italy
[2]Dipartimento di Biologia, Università Roma Tre, 00146 Roma, Italy
[3]Dipartimento di Chimica, Università di Firenze, 50019 Sesto Fiorentino, Italy

(RECEIVED September 6, 2004; FINAL REVISION November 19, 2004; ACCEPTED January 7, 2005)

Abstract

An increasing body of evidence ascribes to misfolded forms of cytochrome *c* (cyt *c*) a role in pathophysiological events such as apoptosis and disease. Here, we examine the conformational changes induced by lipid binding to horse heart cyt *c* at pH 7 and study the ability of ATP (and other nucleotides) to refold several forms of unfolded cyt *c* such as oleic acid-bound cyt *c*, nicked cyt *c*, and acid denatured cyt *c*. The CD and fluorescence spectra demonstrate that cyt *c* unfolded by oleic acid has an intact secondary structure, and a disrupted tertiary structure and heme environment. Furthermore, evidence from the Soret CD, electronic absorption, and resonance Raman spectra indicates the presence of an equilibrium of at least two low-spin species having distinct heme-iron(III) coordination. As a whole, the data indicate that binding of cyt *c* to oleic acid leads to a partially unfolded conformation of the protein, resembling that typical of the molten globule state. Interestingly, the native conformation is almost fully recovered in the presence of ATP or dATP, while other nucleotides, such as GTP, are ineffective. Molecular modeling of ATP binding to cyt *c* and mutagenesis experiments show the interactions of phosphate groups with Lys88 and Arg91, with adenosine ring interaction with Glu62 explaining the unfavorable binding of GTP. The finding that ATP and dATP are unique among the nucleotides in being able to turn non-native states of cyt *c* back to native conformation is discussed in the light of cyt *c* involvement in cell apoptosis.

Keywords: cytochrome *c*; oleic acid; molten globule; nucleotides; resonance Raman spectroscopy

Protein-folding variants, as well as molten globule states have been demonstrated to exist in a living cell (Ptitsyn 1995) and are proposed to have key roles in a number of pathophysiological processes, such as protein recognition by chaperones (Martin and Hartl 1997), protein penetration into membranes (van der Goot et al. 1991) and prion-related disorders (Safar et al. 1998). Recent findings have shown that lipid-induced conformational states of proteins, with structural features resembling those of the molten globule, are active in inducing apoptosis. This is the case of α-lactalbumin bound to oleic acid that possesses spectroscopic properties typical of the molten globule and is able to induce apoptosis in cancer cells (Svensson et al. 1999, 2003; Polverino de Laureto et al. 2002).

In recent years, several non-native conformers of cytochrome *c* (cyt *c*) were characterized, and different biological functions depending on different conformational states of the heme protein were proposed (Cortese et al. 1998; Jemmerson et al. 1999; Nantes et al. 2001; Tuominen et al. 2002; Berezhna et al. 2003; Sivakolundu and Mabrouk 2003). Cyt *c* is well known as a mitochondrial peripheral

Reprint requests to: Laura Fiorucci, Dipartimento di Medicina Sperimentale e Scienze Biochimiche, Università di Roma "Tor Vergata," via Montpellier 1, 00133 Roma, Italy; e-mail: fiorucci@uniroma2.it; fax: +39-0672596477.

Abbreviations: cyt *c*, horse heart cytochrome *c*; cmc, critical micelle concentration; LS, low spin; HS, high-spin; CD, circular dichroism; RR, resonance Raman.

Article published online ahead of print. Article and publication date are at http://www.proteinscience.org/cgi/doi/10.1110/ps.041069405.

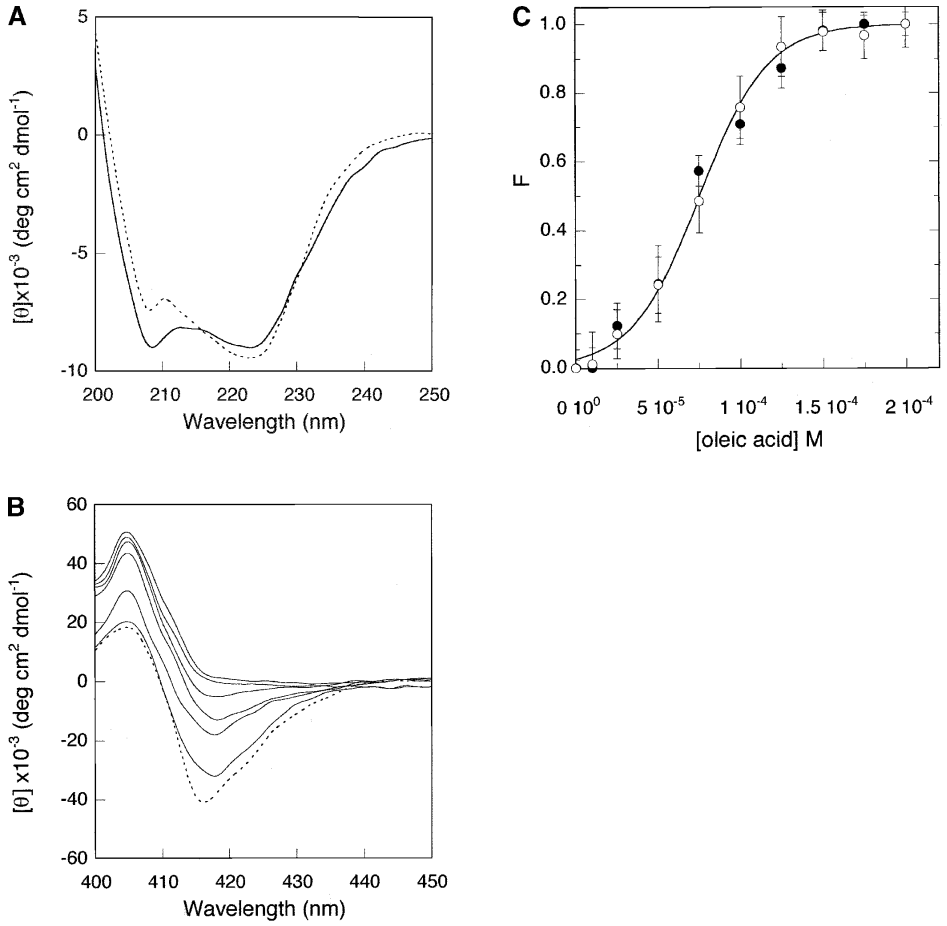

Figure 1. (*A*) Far-UV CD spectrum of cyt *c* alone (. . . .), and in the presence of 150 μM oleic acid (——). (*B*) Soret CD spectrum of cyt *c* alone (. . . .), and in the presence of increasing concentrations of oleic acid up to 200 μM. The concentration of cyt *c* was 7 μM. (*C*) The same data as in *B*, plotted as best fit to a two-state transition, showing the dependence of molar ellipticities, $[\theta]_{416}$ (●) and $[\theta]_{408}$ (○), on the oleic acid concentration. Standard deviations calculated from three different experiments are shown. Experiments were conducted in 10 mM phosphate buffer (pH 7.0) at 25°C. For other details, see text.

membrane protein, localized between the inner and the outer membranes, where it mediates electron transfer between different proteins of the respiratory chain (Pettigrew and Moore 1987). Investigation on the interactions between cyt *c* and various membrane systems suggests that cyt *c* performs electron transfer between cyt *c* reductase and cyt *c* oxidase when it is found in unbound as well as in several membrane-bound non-native conformations, all of which are exchangeable. ATP binds to cyt *c* and can modulate the electron transfer rate with its redox partners (Craig and Wallace 1995), inducing changes in the oxidation state as well as in the thermal stability of free cyt *c* (Craig and Wallace 1991; Antalik and Bagel'ova 1995). Such interactions are compromised when Arg91 is replaced by norleucine (Craig and Wallace 1995; McIntosh et al. 1996; Tuominen et al. 2001).

The recent discovery that cyt *c* plays a role in programmed cell death (apoptosis) after its release from the mitochondrion renewed interest in this protein (Liu et al. 1996; Kluck et al. 1997). Jemmerson et al. (1999) have shown that a membrane-bound form of cyt *c* has apoptotic activity, suggesting that the membrane-associated cyt *c* might be the relevant factor for caspase activation. To form the apoptosome, cyt *c* must interact with Apaf-1, procaspase9 and ATP, or dATP (Green and Reed 1998). Importantly, nucleotide specificity is observed for caspase activation, the cleavage occurring only in the presence of dATP or ATP (Liu et al. 1996; Li et al. 1997). Moreover, particularly interesting is the complete lack of all apoptogenic activity of yeast cytochrome *c*, despite its close structural similarity with mammalian cytochromes *c* (Kluck et al. 2000).

Horse cyt *c* is a single-chain hemoprotein of 104 amino acid residues containing five α-helices, with the prosthetic group lying within a crevice lined with hydrophobic amino acids (Bushnell et al. 1990). The heme is covalently at-

tached to the polypeptide chain by residues Cys14 and Cys17, while His18 and Met80 are the axial ligands of the six-coordinated low-spin heme iron in the native state. In previous studies, limited proteolysis experiments on cyt *c* provided information on partly folded states of the protein. Two stable fragments were obtained and analyzed both separately and mixed together (Santucci et al. 2000b; Sinibaldi et al. 2001; Spolaore et al. 2001). Upon reconstitution, the noncovalent complex showed enhanced flexibility and decreased stability with respect to the native protein, but comparable α-helical content and redox properties.

We report here an investigation of the interaction between ferric cyt *c* and oleic acid and suggest that the fatty acid binding to cyt *c* induces at neutral pH a folding variant with the typical features of a molten globule state. Moreover, we provide evidence that ATP and dATP are unique among the nucleotides in being able to turn non-native states of cyt *c* back to the native conformation and identify a binding site for such nucleotides in horse cytochrome *c* absent in yeast cytochrome *c*.

Results

Characterization of oleic acid-bound cyt c

The far-UV CD spectrum of cyt *c* in the presence of oleic acid, illustrated in Figure 1A, shows the typical features of α-helical protein structure, in which the 222-nm dichroic band is predominantly associated with α-helical n-π* amide transitions. The helical content, determined using the method of Chen et al. (1972) on the basis of the ellipticity values at 222 nm, is ~28% for the complex and 30% for the native protein, indicating the presence of close-ordered secondary structures in both cases. More significant spectral changes upon oleic acid binding are instead present at 208 nm, the dichroic band corresponding to the π-π* amide transitions. Unambiguous interpretation of the spectral changes in this spectral region is not feasible. It was proposed that they might arise from spectral contributions of other secondary structural components (Myer 1968) and/or from the different orientation of aromatic side chains (Manning and Woody 1989). The near UV-CD spectra of cyt *c* in the presence of oleic acid reveal a different protein behavior. In particular, the minimum intensities at 282 and 288 nm, sensitive indicators for the microenvironment of Trp59 (the only tryptophan present in the cyt *c* sequence), decrease as oleic acid concentration is increased up to 200 μM (data not shown).

Integrity of the heme crevice structure of cyt *c* was further monitored in the Soret CD spectrum (400–450 nm) upon increasing the concentration of oleic acid up to 200 μM. A gradual reduction of the CD signal at 416 nm is observed and this spectral change is accompanied by intensification of the 408-nm maximum (Fig. 1B). The intensity of the negative band centered at 416 nm depends on the heme–vicinal residues interaction and decreases when the distance and orientation of the Phe82 side chain, positioned on the Met80 side of the heme plane, are perturbed (Pielak et al. 1986). The isothermal titration correlating the ellipticity values to the oleic acid concentration yields a sigmoidal curve (Fig. 1C) analogous to those from thermal or chemical denaturation (Pace et al. 1989). The fractions of oleic acid-induced species, directly evaluated from the molar ellipticities at 408 and 416 nm, were calculated as $F = ([\theta]_{obs} - [\theta]_N)/([\theta]_{ol} - [\theta]_N)$, where $([\theta]_{obs}$ is the measured molar ellipticity, while $[\theta]_N$ and $[\theta]_{ol}$ are the molar ellipticity values in the native state and oleic acid-induced final state (corresponding to 200 μM fatty acid). The data were analyzed by using a two-state model transition and the ΔG^0 value, i.e., the apparent free-energy change in the absence of oleic acid, was estimated to be 2.1 ± 0.2 Kcal/mol.

The conformation around Trp59 was also investigated by fluorescence spectroscopy (Fig. 2). In native cyt *c* (spectrum a), the Trp59 fluorescence is efficiently quenched by the proximity of the heme group. Under denaturating conditions (Sinibaldi et al. 2001), the fluorescence intensity is strongly enhanced, and shows a maximum at ~350 nm (spectrum e). This change is consistent with a highly hydrated and expanded conformation of the polypeptide chain. The fluorescence increases also upon binding of oleic acid (spectrum c), providing evidence for an increased Trp59-heme iron distance, in agreement with a decreased tertiary packing of this residue, as monitored by the near-UV CD spectrum. The blue shift of about 20 nm observed for the oleic acid-bound cyt *c*, as compared with the emission of the denatured form is indicative of a more solvent-shielded tryptophan.

Effect of nucleotides on oleic acid-bound cyt c

Addition of nucleotides induces no changes in the CD spectrum of free cyt *c* (data not shown), in agreement with

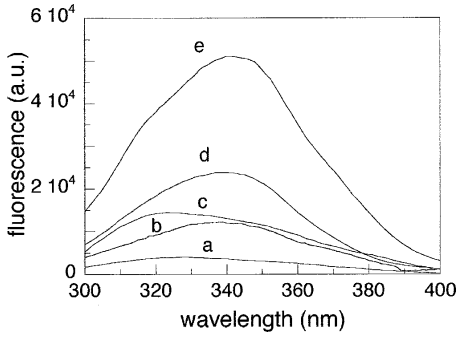

Figure 2. Steady-state fluorescence spectra of native cyt *c* (*a*), nicked cyt *c* (*b*), cyt *c*-oleic acid complex (*c*), acid-denatured cyt *c* at pH 2.2 (*d*), and cyt *c* at pH 7.0 in the presence of 4.0 M GdnHCl (*e*). Cyt *c* and oleic acid concentrations were 7 μM and 150 μM, respectively. The excitation wavelength was 280 nm. Except for the spectra at pH 2.2, experimental conditions are as in Figure 1.

previously reported data (Tuominen et al. 2001). Interestingly, the addition of 3 mM ATP has dramatic consequences on the spectrum of cyt *c* bound to oleic acid, with the recovery of a Soret negative band centered at 412 nm, 4 nm blue-shifted with respect to that native protein (Fig. 3). On adding dATP, the same effect is observed, while GTP, ADP, or CTP produce no changes.

The results of the CD spectroscopy analysis are in agreement with those obtained from electronic absorption measurements and resonance Raman (RR) spectroscopy. The electronic absorption and RR spectra of oxidized cyt *c* alone and in the presence of both oleic acid or oleic acid plus ATP at pH 7 are shown in Figures 4 and 5, respectively. The absorption spectrum of cyt *c* in the presence of oleic acid (Fig. 4) is similar to that of native cyt *c*, except for the band at 695 nm, considered diagnostic for the integrity of the Met 80–Fe(III) bond (Stellwagen and Cass 1974; Santucci and Ascoli 1997), which is reduced in intensity by ~80% (inset, Fig. 4). However, whereas the band intensity recovers by about 60% on adding ATP (inset, Fig. 4) no effect is observed on addition of GTP (data not shown).

The upshift of the RR frequencies of the core size marker bands of cyt *c* in the presence of oleic acid (Fig. 5A, spectrum c) suggests the presence of an alternative LS species with non-native axial iron coordination. A change of axial coordination from Met-His to bis-His for cyt *c*, leading to an upshift of the RR marker band frequencies and reduced intensity of the 695-nm band, has been associated with a more-relaxed heme distortion (Indiani et al. 2000; Zheng et al. 2000). Similar effects have been reported also for the case of His-Lys axial coordination (Dopner et al. 1998; Sinibaldi et al. 2003; Caroppi et al. 2004). The heme of cyt *c* has a pronounced distortion due to interaction with the protein matrix through covalent thioether links between the heme and two cysteine residues (Bushnell et al. 1990; Hu et al. 1993). The heme distortion leads to a very rich RR spectrum in the low-frequency region as out-of-plane modes become active. The intensity and frequency of a number of bands are clearly modified upon addition of oleic acid (Fig. 5B). In particular, the intensities of the out-of-plane modes γ_{22}, γ_{21}, and γ_5 at 445, 566, and 728 cm^{-1}, respectively, are slightly reduced, and changes are evident for vibrations associated with the thioether linkages at 396 cm^{-1} [$\delta(C_\beta C_aS)$] and 692 cm^{-1} ν(C-S) and the ν_7 mode at 700 cm^{-1} (spectrum c). Similar changes have been observed previously for cyt *c*, following a change of axial coordination that results in a less-distorted heme (Smulevich et al 1994; Jordan et al. 1995; Indiani et al. 2000; Zheng et al. 2000). Hence, as inferred from the high-frequency spectra, the variations observed in the low frequency spectra of cyt *c* in the presence of oleic acid also indicate a structural rearrangement leading to a change of axial ligand. The nature of the non-native ligand in the alternative low-spin state is expected to be a histidine (His26, His33) or lysine (Lys72, Lys73, Lys79) residue. Recently, analysis of the low frequency region (390–420 cm^{-1}) of the RR spectrum of a noncovalent complex reconstituted upon mixing two noncontiguous fragments of cyt *c* proved to be decisive in distinguishing between a Met, Lys, or His ligand bound to the heme iron (Caroppi et al. 2004). In the present case, the changes in intensity and frequency of the $\delta(C_\beta C_aS)$ band at 396 cm^{-1} and the δ ($C_\beta C_aC_b$) band at 413 cm^{-1} upon addition of oleic acid to cyt *c* are not consistent with the changes observed when cyt *c* adopts bis-His coordination (Santoni et al. 2004), where a significant intensity increase of a δ ($C_\beta C_aC_b$)

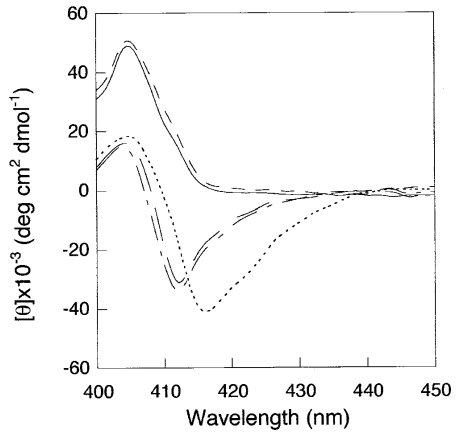

Figure 3. Soret CD spectra of the cyt *c*-oleic acid complex in the presence of nucleotides. Cyt *c* 7 μM alone (. . . .), in the presence of oleic acid (150 μM) (——), and upon addition of 3 mM ATP (— —), dATP (---) or GTP (----). Experimental conditions are as in Figure 1.

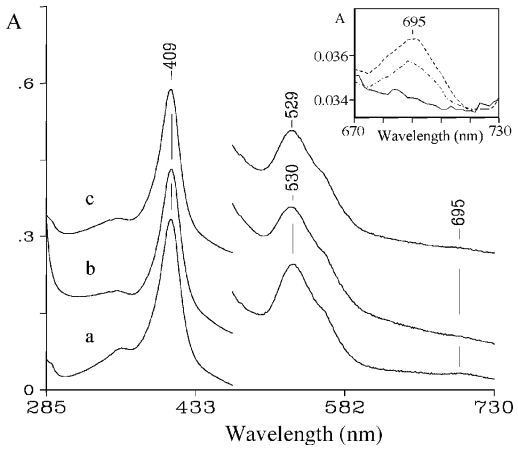

Figure 4. Electronic absorption spectra of native cyt *c* alone (*a*), in the presence of 0.7 mM oleic acid and 3 mM ATP (*b*), and in the presence of 0.7 mM oleic acid only (*c*). Experimental conditions: sample concentration, 30 μM; 10 mM phosphate buffer (pH 7.0) at 25°C. The visible region is expanded sixfold. The path length of the cuvette was 1 mm for all spectra. The ordinate axis scale refers to spectrum a. In the *inset*, the electronic absorption spectra of cyt *c* in the 670–730 nm range in the presence of oleic acid (——) and oleic acid plus 3 mM ATP (-·-·) are shown. The spectrum of native cyt *c* (----) is shown for comparison.

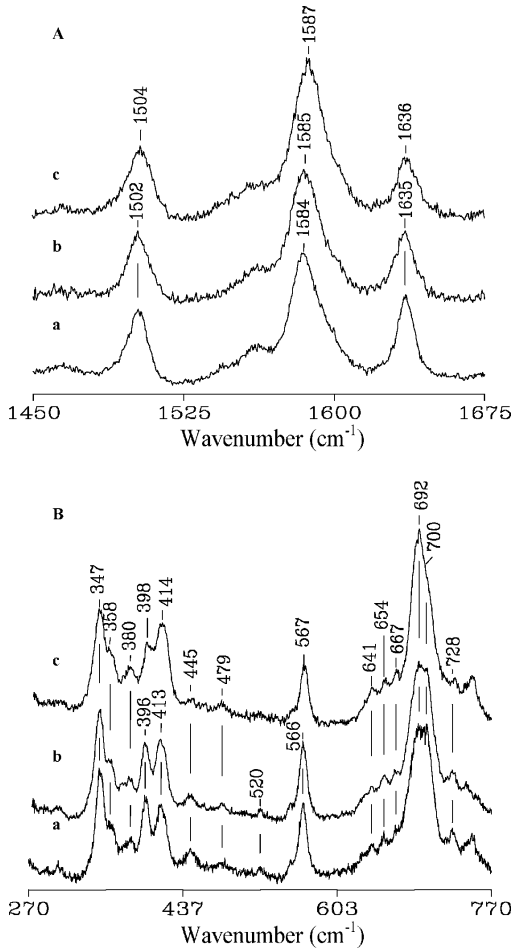

Figure 5. Resonance Raman spectra of native cyt *c* alone (*a*), in the presence of 0.7 mM oleic acid and 3 mM ATP (*b*), and in the presence of 0.7 mM oleic acid only (*c*) in 10 mM phosphate (pH 7.0). Experimental conditions: sample concentration, 30 μM; 5 cm^{-1} resolution; 406.7 nm excitation; 15 mW laser power at the sample. (*A*) High-frequency region: (*a*) 6 sec/0.5 cm^{-1} collection interval; (*b*) 8 sec/0.5 cm^{-1} collection interval; (*c*) 10 sec/0.5 cm^{-1} collection interval. (*B*) Low-frequency region: (*a*) 3 sec/0.5 cm^{-1} collection interval; (*b*) 6 sec/0.5 cm^{-1} collection interval; (*c*) 4 sec/0.5 cm^{-1} collection interval.

band at 418 cm^{-1} is expected. On the contrary, they are similar to those observed following the alkaline transition of cyt *c* (Dopner et al. 1999), characterized by two conformers, in which Lys73 or Lys79 replaces the axial Met ligand bound to the heme iron at neutral pH. Only the alkaline conformer with Lys73 bound to the heme iron has significantly different spectral characteristics with respect to the neutral form (Dopner et al. 1998), the Lys79-bound alkaline conformer being very similar to the neutral form. Hence, although a small contribution from a bis-His state cannot be excluded, it is suggested that Lys73 is the misligated ligand in the presence of oleic acid. Addition of ATP to the sample of cyt *c* plus oleic acid leads to RR spectra closely similar to those of the native protein (Fig. 5, spectra b). This indicates that ATP reverses the changes induced by oleic acid almost completely. It must be noted that spectra identical to those reported in Figures 4 and 5 were obtained when using lower concentrations of cyt *c* (15 μM) and oleic acid (500 μM).

Effect of nucleotides on the conformational states of cyt c *induced by pH and backbone cleavage*

The spectrum of the (1–56/57–104 residues) fragment complex of cyt *c* (so-called nicked cyt *c*) showed a weak Cotton effect at 416 nm (Sinibaldi et al. 2001; Spolaore et al. 2001), consistent with an altered, less-packed tertiary conformation, at least in the heme pocket region, when compared with native cyt *c* (Fig. 6). Addition of 3 mM ATP enhanced the 416-nm Cotton effect to a value close to that typical of native cyt *c* (although a 2-nm blue shift is observed). Therefore, addition of ATP completely restores the native conformation of cyt *c*, indicating that the nucleotide has a stabilizing effect on the protein. As expected, no effect was observed (data not shown) when ATP is added to the unstructured N-terminal fragment (1–56 residues) (Santucci et al. 2000b). Furthermore, ATP (or dATP) causes a similar effect (in contrast with GTP that is ineffective) when added to acid-denaturated cyt *c* at pH 2.2.

Identification of binding site of ATP by docking simulations and mutagenesis experiments

Figure 7 shows the putative cyt *c*–ATP complex obtained by docking simulations. Several specific interactions between ATP and cyt *c* can be observed. In detail, the adenine moiety is bound in a slight depression of the cyt *c* molecular surface with its NH_2 group interacting with the carboxyl group of Glu62. The phosphate groups of ATP in turn es-

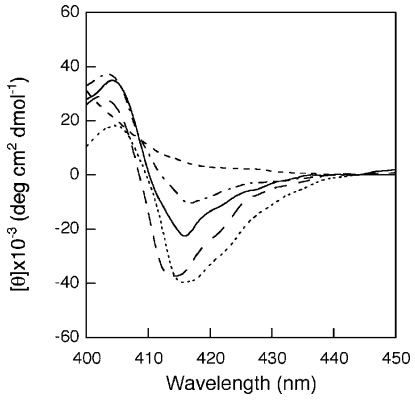

Figure 6. Soret CD spectra of nicked cyt *c* at pH 7.0 alone (——) and after addition of 3 mM ATP (— —), acid-denatured cyt *c* at pH 2.2 alone (----) and after addition of 3 mM ATP (-·-·). Cyt *c* (. . . .) is shown for comparison. Cyt *c* concentration was 7 μM. Other conditions are as for Figure 1.

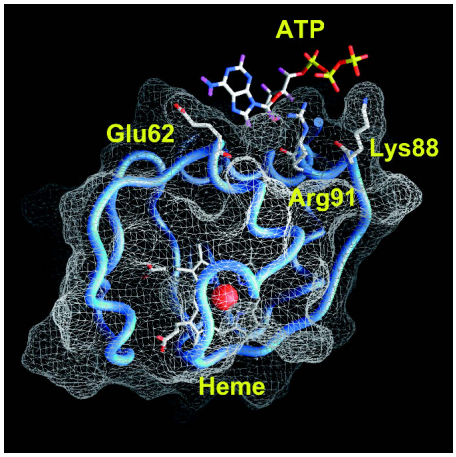

Figure 7. Schematic representation of the cyt *c*–ATP complex obtained by a docking simulations (see Materials and Methods), showing the ATP-binding site with respect to the heme pocket. The iron atom is represented by a red sphere. Residues shown are those having electrostatic interactions with the amine group (Glu62) and the phosphate groups (Lys88 and Arg91) of ATP. The figure was made with Grasp (Nicholls et al. 1991).

tablish strong electrostatic interactions with the basic side chains of Arg91 and Lys88. The calculated binding energy for the complex formation is −5.2 kcal/mol, equivalent to a binding constant (Kd) of 1.7×10^{-4} M. This value is consistent with the observation of an effect on the CD spectrum of cyt *c* bound to oleic acid upon addition of ATP in the millimolar concentration range. It is worthwhile to note that docking of GTP with cyt *c* did not yield any complex of comparable binding energy. The lowest energy complex of GTP with cyt *c* in the vicinity of Arg91 is, in fact, characterized by a binding-free energy of −2.2 kcal/mol, yielding a kilodalton value more than two orders of magnitude higher with respect to that calculated for the ATP-cyt *c* complex. The experiments described in Figure 3 have been repeated with *Escherichia coli*-expressed wild-type iso-1 cyt *c* plus oleic acid and ATP. They demonstrate the inability of the nucleotide to refold the non-native conformation of cyt *c* induced by oleic acid (Fig. 8). To test whether the absence of Glu62 and Lys88, replaced in the iso-1 cyt *c* sequence with Asn and Glu, respectively (Narita and Chitani 1969) is responsible for the lack of interaction between iso-1 cyt *c* and ATP, we generated the *E. coli*-expressed Asn62Glu/Glu88Lys iso-1 cyt *c* double mutant. As predicted by docking simulations, ATP now interacts with the iso-1 cyt *c* variant in that it is able to partially refold the oleic acid-bound cyt *c* (Fig. 8).

Discussion

All of the results reported in this study indicate that oleic acid induces structural changes to cyt *c* when used at concentrations below the cmc. Such conformational changes are probably related to the formation of a molten globule-like state, i.e., a compact state possessing native-like secondary structure but fluctuating tertiary conformation. The spectral changes detected in the near-UV and visible region by CD, fluorescence, electronic, and RR spectroscopies reveal that a conformational rearrangement in the tertiary structure of the protein occurs in the presence of oleic acid. The protein tertiary structure becomes less compact, and the strength of the Met80 bond to Fe(III) decreases considerably. No spin-state change is observed, the protein maintains a low-spin configuration, and the metal is hexa-coordinated. According to previous reports (Dopner et al. 1998; Indiani et al. 2000; Zheng et al. 2000; Sinibaldi et al. 2003; Caroppi et al. 2004), CD, electronic absorption, and RR data are consistent with the presence of a mixed population in solution composed of at least two low-spin species, the first retaining the Met80 native ligand, whereas the other is characterized by an alternative endogenous side chain bound to the metal (a lysine rather than histidine residue is favored). The binding of monomeric oleic acid to cyt *c* is believed to involve electrostatic and hydrophobic sites. Previous results (Rytomaa and Kinnunen 1995; Stewart et al. 2000) have suggested that binding of deprotonated free fatty to cyt *c* involves electrostatic interactions with basic residues on the surface of the protein, in particular with Lys72 that belongs to the ring of lysines located around the exposed heme edge. A further interaction of the acyl chain with a hydrophobic channel leading from the surface of the protein to the heme crevice might cause the disruption of the S-Fe coordination between Met80 and the heme iron. Moreover, analysis of the three-dimensional structure of cyt *c* (Bushnell et al. 1990) reveals the presence of surface hydrophobic domains,

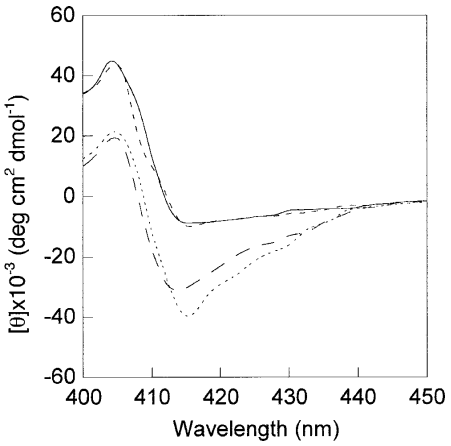

Figure 8. Soret CD spectra of the Asn62Glu/Glu88Lys iso-1-cyt *c* mutant 7 μM alone (. . . .), in the presence of oleic acid (100 μM) (——) and upon addition of 3 mM ATP (— —). Soret CD spectra of the wild-type iso-1-cyt *c* alone and in the presence of oleic acid are identical to the corresponding mutant spectra. The addition of ATP does not change the spectrum of the wild-type iso-1-cyt *c*-oleic acid complex (----). Experimental conditions are as in Figure 1.

which can interact with the oleic acid acyl chain. In particular, the segment constituted by residues 85–81 is directly linked to the axial Met80 ligand of the heme. Thus, the hydrophobic binding of monomeric oleic acid to cyt *c* in this region may pull away the 70–85 residue polypeptide segment, promoting the weakening or rupture of the Met80-Fe(III) axial bond. Such an interaction mechanism has been previously suggested for the binding of cyt *c* and SDS monomer, which induces the conversion of native cyt *c* to a putative functionally relevant B2 state. This state is one of two conformers (B1 and B2), which are observed for cyt *c* bound to phospholipid vesicles, and is characterized by dissociation of the axial Met80 ligand (Hildebrandt et al. 1990; Dopner et al. 1999; Oellerich et al. 2003). A second hydrophobic patch that represents a potential interaction site for the hydrophobic acyl chain of the fatty acid is the 43–46 segment. Interestingly, the dichroic spectrum of cyt *c* in 150 μM oleic acid is similar to that of the cyt *c* molten globule state at neutral pH described for the His26Tyr mutant (Sinibaldi et al. 2003), which was induced by the loss of the hydrogen bond between the His26 and Pro44 residues that bridges the 20s and 40s Ω-loops in the native protein (Bushnell et al. 1990). In fact, the hydrophobic interaction of the oleic acid acyl chain with the 43–46 cyt *c* residue segment may contribute to the rupture of the hydrogen bond, thereby enhancing the fluctuations of the two loops, leading to a weakening of the Met80-Fe(III) axial bond. In keeping with these observations, perturbation of Trp59 packing and the increasing Trp59-heme distance (as probed by CD and fluorescence measurements) are consistent with a partial unfolding of cyt *c*. The change in the Trp environment on going from the compact, native cyt *c* to the expanded conformation of acid-denaturated cyt *c* is characterized by an increase of fluorescence intensity. The oleic acid cyt *c* complex has a fluorescence intensity weaker than the acid-denatured cyt *c*, but comparable to that of nicked cyt *c*, a native-like complex in which Trp59 experiences a local enhanced flexibility, being close to the cleavage site of the polypeptide chain (Gly56-Ile57 peptide bond) (Sinibaldi et al. 2001).

On the whole, the experiments described here suggest that oleic acid-bound cyt *c* is likely to have a disrupted Met80-heme ligation, an expanded Trp59-heme distance, and retention of a native-like α-helical structure, all features characteristic of the molten globule state of cyt *c*. In fact, although the measurements probe changes in the heme environment, such changes reflect long-range effects provoked by oleic acid. In particular, it is suggested that Lys73 binds to the heme iron in the presence of oleic acid, implicitly revealing a rearrangement of the protein fold in the misligated conformer and enhanced mobility of the Met80-containing loop. As suggested by Hoang et al. (2003), in order to physically remove Met80 from the heme and replace it with one of the surface lysine residues, this segment must necessarily deviate from the native structure, with the prior (or contemporary) unfolding of the 40s Ω loop (Krishna et al. 2004). The formation of a molten globule state upon binding of Lys to the heme iron of cyt *c* has been reported previously (Sinibaldi et al. 2003). Interestingly, lipid binding to α-lactalbumin has been suggested to induce the molten globule state (Polverino de Laureto et al. 2002). In this regard, it is worth noting that α-lactalbumin with bound oleic acid has been recently reported to induce apoptosis in cancer cells (Svensson et al. 1999, 2003). Analogously, structural changes of cyt *c* in apoptotic cell death were related to those induced in the complex formed with the phospholipid vesicles. Such changes include alterations of the tertiary structure and perturbation of the heme crevice (Pinheiro et al. 1997; Oellerich et al. 2002). In particular, it was suggested (Jemmerson et al. 1999) that a membrane-bound conformationally altered form of cyt *c* might be the relevant form in caspase activation. The authors found that antibodies recognizing apoptotic cyt *c* specifically interact with the region around Pro44. Considering that cyt *c* interacts with APAF-1, dATP, or ATP and pro-caspase in the cytosol to form an apoptosome, it is immediately apparent that a mechanism for cyt *c* translocation to cytosolic states must exist. Accordingly, in the light of the evidence pointing to ferricyt *c* as the caspase activator in the cytosol (Ghafourifar et al. 1999; Pan et al. 1999), we considered that useful insight could be gained by investigating the interaction of ferricyt *c* with nucleotides. Importantly, among the nucleotides tested, only ATP and dATP are able to restore the structural features of native cyt *c* in the presence of oleic acid. CD, electronic absorption, and RR spectroscopies demonstrate that the less-organized tertiary structure induced upon binding of cyt *c* to oleic acid is converted back to the native state by adding ATP and dATP at millimolar concentrations. Indeed, the concentration range of ATP present in the cytoplasm of living cells is millimolar (Skoog and Bjursell 1974), sufficient for it to bind to cyt *c* (Craig and Wallace 1991), in agreement with the binding constant (Kd) evaluated by docking simulation experiments. Furthermore, ATP, but not GTP, is effective in completely restoring the native conformation in a nicked form of cyt *c* and, at millimolar concentration, ATP leads to a Soret CD spectrum of acid-denaturated cyt *c* at pH 2.2 similar to that of the anion-induced A state of cyt *c* (Goto et al. 1990; Santucci et al. 2000a). Our findings demonstrate that nucleotides have a markedly different capacity to revert non-native states of cyt *c* back to the native conformation, with ATP and dATP being the only ones effective. In addition, docking simulations suggest a further explanation for the capacity of ATP, but not GTP, to cause reversion of non-native states of cyt *c* into the native conformation. In fact, at variance with the adenosine moiety, guanosine would be unable to establish interactions with the Glu62 side chain. Thus, the conclusions of the spectroscopic studies and the ATP, GTP docking simulations are in full agreement, revealing that cyt *c*

has a much greater affinity for ATP than GTP. These observations suggest that the exclusive requirement for ATP or dATP in cyt *c*-mediated apoptosis (Liu et al. 1996; Li et al. 1997) is related to their capacity to alter the conformation of the protein. It is therefore tempting to speculate that the binding of ATP to lipid-bound cyt *c* is important in restoring a cyt *c* conformation suitable for the interaction with Apaf-1 and pro-caspase 9 to form the apoptosome. Interestingly, the amino acid residues here identified as involved in the interaction of ATP with cyt *c*, Glu62, and Lys88, are replaced by Asn and Glu, respectively, in cyt *c* from the yeast *Saccharomyces cerevisiae* that lacks pro-apoptotic activity (Kluck et al. 2000). A yeast cytochrome *c* double mutant, containing modifications at the Asn62 and Glu88 sites to mimic the horse heart cytochrome *c* sequence, indeed confirms the importance of such residues in the binding of ATP.

Materials and methods

Materials

Horse heart cytochrome *c* (type VI), oleic acid, thermolysin, and nucleotides were obtained from Sigma. All other reagents were of analytical grade.

Sample preparation

To prepare the oleic acid solution, a weighed amount of fatty acid was dissolved in 1 mL of ethanol and then diluted to the desired concentration with the appropriate buffer. The concentrations of oleic acid used in this study were below the published micelle concentration (cmc) that has been reported to be in the range 0.72–2 mM (Mukerjee and Mysels 1971; Stewart et al. 1991).

Acid-unfolded cyt *c* was prepared by diluting a concentrated H_2O solution of cyt *c* into an aqueous HCl solution (pH 2.2).

Digestion of cyt *c* and purification of N-terminal fragment (1–56 residues) and C-terminal fragment (57–104 residues), as well as cyt *c* complex reconstitution have been performed as previously described (Sinibaldi et al. 2001; Spolaore et al. 2001) to obtain the so-called nicked cyt *c*.

The expression plasmid pBTRI harboring the yeast (C102T) iso-1-cyt *c* gene was a kind gift from Dr. A. Grant Mauk (British Columbia University at Vancouver, Canada). Site-directed mutagenesis was performed directly on the pBTRI plasmid. Specific amino acid substitutions (Asn62Glu and Glu88Lys) were introduced in iso-1-cyt *c* gene using the QuikChange "In Vitro Site Directed Mutagenesis Kit" (Stratagene) following the manufacturer's instructions. Growth of *E. coli* JM 109 strain containing the BPTR1 plasmid and purification of cytochrome *c* were performed as described previously (Sinibaldi et al. 2003). The purified stocks of cytochrome *c* were concentrated (100 μM) and stored at −80°C until needed.

Circular dichroism spectroscopy

CD spectra in the far-UV (200–250 nm) as well as in the near-UV (260–300 nm) and in the Soret (400–450 nm) regions were recorded on a Jasco-710 spectropolarimeter equipped with a PC as data processor and a temperature-controlled holder maintained at 25°C. Quartz cells with 1- and 5- mm light paths were used for measurements in the far-UV and in the near-UV/Soret regions, respectively. Spectra were obtained for samples containing 7 μM cyt *c* in the absence and presence of different concentrations of oleic acid (up to 200 μM) and nucleotides, as indicated in the figure legends. Spectra in the Soret region were also obtained for samples containing 7 μM nicked cyt *c* in 0.01 M phosphate buffer (pH 7.0) and for acid-denaturated cyt *c* in the absence and the presence of 150 μM oleic acid and nucleotides. Moreover, Soret CD spectra were recorded for samples containing 7 μM *E. coli*-expressed wild-type iso-1 cyt *c* and *E. coli*-expressed Asn62Glu/Glu88Lys iso-1 cyt *c* double mutant in the absence and the presence of 100 μM oleic acid and 3 mM ATP (for other details, see figure legends). All spectra were corrected subtracting their corresponding backgrounds. The molar ellipticity ($deg*cm^2*dmol^{-1}$) is expressed as $[\theta]_h$ on a molar heme basis in the Soret and near UV regions and as mean residue ellipticity $[\theta]_a$ in the far-UV region (mean residue relative molecular mass = 119 g/mol). Spectra were acquired with 0.5 nm/min resolution and four scans were averaged per spectrum.

The analysis of the transition profile from native cyt *c* to the conformational state induced by oleic acid was performed according to a two-state model transition, assuming a linear dependence of the free energy change on the oleic acid concentration.

Steady-state fluorescence

Fluorescence spectra were measured at room temperature on a ISS K2 spectrofluorimeter. Samples contained 7 μM cyt *c* or cyt *c* bound to 150 μM oleic acid in 0.01 M phosphate buffer. Spectra of 7 μM nicked cyt *c*, acid-denaturated cyt *c*, and GdnHCl-denaturated cyt *c* were also measured. The excitation and emission bandwidths were $\Delta\lambda = \pm 4$ nm and an excitation wavelength of $\lambda = 280$ nm was used. All spectra were corrected for the corresponding backgrounds.

Electronic absorption and resonance Raman measurements

Electronic absorption measurements were carried out at 25°C using a Cary 5 spectrophotometer. Cyt *c* concentration was determined on the basis of the extinction coefficient $\varepsilon = 106\ mM^{-1}\ cm^{-1}$ at 408 nm. Resonance Raman (RR) spectra were obtained at room temperature with excitation from the 406.7-nm line of a Kr^+ laser (Coherent, Innova 302C). The back-scattered light from a slowly rotating NMR tube was collected and focused into a computer-controlled double monochromator (Jobin-Yvon HG2S) equipped with a cooled photomultiplier (RCA C31034A) and photon counting electronics. To minimize local heating of the protein by the laser beam, the sample was cooled by a gentle flow of N_2 gas passed through liquid N_2. RR spectra were calibrated to an accuracy of 1 cm^{-1} for intense isolated bands, with indene as the standard for the high-frequency region and with indene and CCl_4 for the low-frequency region. Samples in the presence of oleic acid and ATP were prepared by addition of aliquots of stock solutions of oleic acid (70.8 mM) and ATP (400 mM) to obtain final concentrations of 0.7 and 3 mM, respectively.

Docking simulations

ATP and GTP were docked on the oxidized horse heart cyt *c* three-dimensional structure (PDB code 1AKK; Banci et al. 1997)

using the program AutoDock 3.0, which allows docking of flexible ligands on target macromolecules using a lamarkian genetic algorithm (Morris et al. 1998). In detail, ligands were allowed to explore their conformational space, while cyt *c* conformation was kept fixed. The procedure yielded 100 different complexes for each ligand, and both the binding-free energy and the ligand intramolecular energy were evaluated. As far as ATP is concerned, available experimental data indicate that binding of this nucleotide to cyt *c* is compromised by replacement of Arg91 by norleucine (Craig and Wallace 1995; McIntosh et al. 1996; Tuominen et al. 2001). Thus, among the complexes obtained, only those consistent with the binding of ATP in the vicinity of Arg91 were further analyzed. Among them, the complex displaying the lowest binding energy is described in the Results section.

Acknowledgments

We thank Dr. A. Grant Mauk (British Columbia University at Vancouver, Canada) for supplying the yeast iso-1-cyt *c* expression plasmid. This research was funded in part by a grant from Italian MIUR (PRIN 2004, prot. 2004055484).

References

Antalik, M. and Bagel'ova, J. 1995. Effect of nucleotides on thermal stability of ferricytochrome *c*. *Gen. Physiol. Biophys.* **14:** 19–37.

Banci, L., Bertini, I., Gray, H.B., Luchinat, C., Reddig, T., Rosato, A., and Turano, P. 1997. Solution structure of oxidized horse heart cytochrome *c*. *Biochemistry* **36:** 9867–9877.

Berezhna, S., Wohlrab, H., and Champion, P.M. 2003. Resonance Raman investigations of cytochrome *c* conformational change upon interaction with the membranes of intact and Ca^{2+}-exposed mitochondria. *Biochemistry* **42:** 6149–6158.

Bushnell, G.W., Louie, G.V., and Brayer, G.D. 1990. High-resolution three-dimensional structure of horse heart cytochrome *c*. *J. Mol. Biol.* **214:** 585–595.

Caroppi, P., Sinibaldi, F., Santoni, E., Howes, B.D., Fiorucci, L., Ferri, T., Ascoli, F., Smulevich, G., and Santucci, R. 2004. The 40s Ω-loop plays a critical role in the stability and the alkaline conformational transition of cytochrome *c*. *J. Biol. Inorg. Chem* **9:** 997–1006.

Chen, Y.H., Yang, J.T., and Martinez, H.M. 1972. Determination of the secondary structures of proteins by circular dichroism and optical rotatory dispersion. *Biochemistry* **11:** 4120–4131.

Cortese, J.D., Voglino, A.L., and Hackenbrock, C.R. 1998. Multiple conformations of physiological membrane-bound cytochrome *c*. *Biochemistry* **37:** 6402–6409.

Craig, D.B. and Wallace, C.J. 1991. The specificity and Kd at physiological ionic strength of an ATP-binding site on cytochrome *c* suit it to a regulatory role. *Biochem. J.* **279:** 781–786.

———. 1995. Studies of 8-azido-ATP adducts reveal two mechanisms by which ATP binding to cytochrome *c* could inhibit respiration. *Biochemistry* **34:** 2686–2693.

Dopner, S., Hildebrandt, P., Rosell, F.I., and Mauk, A.G. 1998. Alkaline conformational transitions of ferricytochrome *c* studied by resonance raman spectroscopy. *J. Am. Chem. Soc.* **120:** 11246–11255.

Dopner, S., Hildebrandt, P., Rosell, F.I., Mauk, A.G., von Walter, M., Buse, G., and Soulimane, T. 1999. The structural and functional role of lysine residues in the binding domain of cytochrome *c* in the electron transfer to cytochrome *c* oxidase. *Eur. J. Biochem.* **261:** 379–391.

Ghafourifar, P., Klein, S.D., Schucht, O., Schenk, U., Pruschy, M., Rocha, S., and Richter, C. 1999. Ceramide induces cytochrome *c* release from isolated mitochondria. Importance of mitochondrial redox state. *J. Biol. Chem.* **274:** 6080–6084.

Goto, Y., Takahashi, N., and Fink, A.L. 1990. Mechanism of acid-induced folding of proteins. *Biochemistry* **29:** 3480–3488.

Green, D.R. and Reed, J.C. 1998. Mitochondria and apoptosis. *Science* **281:**1309–1312.

Hildebrandt, P., Heimburg, T., and Marsh, D. 1990. Quantitative conformational analysis of cytochrome *c* bound to phospholipid vesicles studied by resonance Raman spectroscopy. *Eur. Biophys. J.* **18:** 193–201.

Hoang, L., Maity, H., Krishna, M.M., Lin, Y., and Englander, S.W. 2003. Folding units govern the cytochrome *c* alkaline transition. *J. Mol. Biol.* **331:** 37–43.

Hu, S., Morris, I.K., Singh, J.P., Smith, K.M., and Spiro, T.G. 1993. Complete assignment of cytochrome *c* resonance Raman spectra via enzymic reconstitution with isotopically labeled hemes. *J. Am. Chem. Soc.* **115:** 12446–12458.

Indiani, C., De Sanctis, G., Neri, F., Santos, H., Smulevich, G., and Coletta, M. 2000. Effect of pH on axial ligand coordination of cytochrome *c″* from *Methylophilus methylotrophus* and horse heart cytochrome *c*. *Biochemistry* **39:** 8234–8242.

Jemmerson, R., Liu, J., Hausauer, D., Lam, K.P., Mondino, A., and Nelson, R.D. 1999. A conformational change in cytochrome *c* of apoptotic and necrotic cells is detected by monoclonal antibody binding and mimicked by association of the native antigen with synthetic phospholipid vesicles. *Biochemistry* **38:** 3599–3609.

Jordan, T., Eads, J.C., and Spiro, T.G. 1995. Secondary and tertiary structure of the A-state of cytochrome *c* from resonance Raman spectroscopy. *Protein Sci.* **4:** 716–728.

Kluck, R.M., Bossy-Wetzel, E., Green, D.R., and Newmeyer, D.D. 1997. The release of cytochrome *c* from mitochondria: A primary site for Bcl-2 regulation of apoptosis. *Science* **275:** 1132–1136.

Kluck, R.M., Ellerby, L.M., Ellerby, H.M., Naiem, S., Yaffe, M.P., Margoliash, E., Bredesen, D., Mauk, A.G., Sherman, F., and Newmeyer, D.D. 2000. Determinants of cytochrome *c* pro-apoptotic activity. The role of lysine 72 trimethylation. *J. Biol. Chem.* **275:** 16127–16133.

Krishna, M.M., Lin, Y., and Englander, S.W. 2004. Protein misfolding: Optional barriers, misfolded intermediates, and pathway heterogeneity. *J. Mol. Biol.* **343:** 1095–1109.

Li, P., Nijhawan, D., Budihardjo, I., Srinivasula, S.M., Ahmad, M., Alnemri, E.S., and Wang, X. 1997. Cytochrome *c* and dATP-dependent formation of Apaf-1/caspase-9 complex initiates an apoptotic protease cascade. *Cell* **91:** 479–489.

Liu, X., Kim, C.N., Yang, J., Jemmerson, R., and Wang, X. 1996. Induction of apoptotic program in cell-free extracts: Requirement for dATP and cytochrome *c*. *Cell* **86:** 147–157.

Manning, M.C. and Woody, R.W. 1989. Theoretical study of the contribution of aromatic side chains to the circular dichroism of basic bovine pancreatic trypsin inhibitor. *Biochemistry* **28:** 8609–8613.

Martin, J. and Hartl, F.U. 1997. Chaperone-assisted protein folding. *Curr. Opin. Struct. Biol.* **7:** 41–52.

McIntosh, D.B., Parrish, J.C., and Wallace, C.J. 1996. Definition of a nucleotide binding site on cytochrome *c* by photoaffinity labeling. *J. Biol. Chem.* **271:** 18379–18386.

Morris, G.M., Goodsell, D.S., Halliday, R.S., Huey, R., Hart, W.E., Belew, R.K., and Olson, A.J. 1998. Automated docking using a Lamarckian genetic algorithm and an empirical binding free energy function. *J. Comput. Chem.* **19:** 1639–1662.

Mukerjee, P. and Mysels, K.J. 1971. National Bureau of Standards, Washington, DC.

Myer, Y.P. 1968. Far ultraviolet circular dichroism spectra of cytochrome *c*. *Biochim. Biophys. Acta* **154:** 84–90.

Nantes, I.L., Zucchi, M.R., Nascimento, O.R., and Faljoni-Alario, A. 2001. Effect of heme iron valence state on the conformation of cytochrome *c* and its association with membrane interfaces. A CD and EPR investigation. *J. Biol. Chem.* **276:** 153–158.

Narita, K. and Chitani, K. 1969. The complete amino acid sequence in baker's yeast cytochrome *c*. *J. Biochem.* **65:** 259–267.

Nicholls, A., Sharp, K.A., and Honig, B. 1991. Protein folding and association: Insights from the interfacial and thermodynamic properties of hydrocarbons. *Proteins* **11:** 281–296.

Oellerich, S., Wackerbarth, H., and Hildebrandt, P. 2002. Spectroscopic characterization of non-native conformational states of cytochrome *c*. *J. Phys. Chem. B* **106:** 6566–6580.

———. 2003. Conformational equilibria and dynamics of cytochrome *c* induced by binding of sodium dodecyl sulfate monomers and micelles. *Eur. Biophys. J.* **32:** 599–613.

Pace, C.N., Shirley, B.A., and Thomson, J.A. 1989. Measuring the conformational stability of a protein. In *Protein structure: A practical approach* (ed. T.E. Creighton), pp. 311–330. IRL Press at Oxford University Press, Oxford, UK.

Pan, Z., Voehringer, D.W., and Meyn, R.E. 1999. Analysis of redox regulation of cytochrome *c*-induced apoptosis in a cell-free system. *Cell Death Differ.* **6:** 683–688.

Pettigrew, G.W. and Moore, G.R. 1987. *Cytochromes c: Biological aspects.* Springer, Berlin.

Pielak, G.J., Oikawa, K., Mauk, A.G., Smith, M., and Kay, C.M. 1986. Elimination of the negative soret Cotton effect of cytochrome *c* by replacement of the invariant phenylalanine using site-directed mutagenesis. *J. Am. Chem. Soc.* **108:** 2724–2727.

Pinheiro, T.J., Elove, G.A., Watts, A., and Roder, H. 1997. Ceramide induces cytochrome *c* release from isolated mitochondria. Importance of mitochondrial redox state. *Biochemistry* **36:** 13122–13132.

Polverino de Laureto, P., Frare, E., Gottardo, R., and Fontana, A. 2002. Molten globule of bovine α-lactalbumin at neutral pH induced by heat, trifluoroethanol, and oleic acid: A comparative analysis by circular dichroism spectroscopy and limited proteolysis. *Proteins* **49:** 385–397.

Ptitsyn, O.B. 1995. Molten globule and protein folding. *Adv. Protein. Chem.* **47:** 83–229.

Rytomaa, M. and Kinnunen, P.K. 1995. Reversibility of the binding of cytochrome *c* to liposomes. Implications for lipid-protein interactions. *J. Biol. Chem.* **270:** 3197–3202.

Safar, J., Wille, H., Itri, V., Groth, D., Serban, H., Torchia, M., Cohen, F.E., and Prusiner, S.B. 1998. Eight prion strains have PrP(Sc) molecules with different conformations. *Nat. Med.* **4:** 1157–1165.

Santoni, E., Scatragli, S., Sinibaldi, F., Fiorucci, L., Santucci, R., and Smulevich, G. 2004. A model for the misfolded bis-His intermediate of cytochrome *c*: The 1–56 N-fragment. *J. Inorg. Biochem.* **98:** 1067–1077.

Santucci, R. and Ascoli, F. 1997. The Soret circular dichroism spectrum as a probe for the heme Fe(III)-Met(80) axial bond in horse cytochrome *c*. *J. Inorg. Biochem.* **68:** 211–214.

Santucci, R., Bongiovanni, C., Mei, G., Ferri, T., Polizio, F. and Desideri, A. 2000a. Anion size modulates the structure of the A state of cytochrome *c*. *Biochemistry* **39:** 12632–12638.

Santucci, R., Fiorucci, L., Sinibaldi, F., Polizio, F., Desideri, A., and Ascoli, F. 2000b. The heme-containing N-fragment (residues 1–56) of cytochrome *c* is a bis-histidine functional system. *Arch. Biochem. Biophys.* **379:** 331–336.

Sinibaldi, F., Fiorucci, L., Mei, G., Ferri, T., Desideri, A., Ascoli, F., and Santucci, R. 2001. Cytochrome *c* reconstituted from two peptide fragments displays native-like redox properties. *Eur. J. Biochem.* **268:** 4537–4543.

Sinibaldi, F., Piro, M.C., Howes, B.D., Smulevich, G., Ascoli, F., and Santucci, R. 2003. Rupture of the hydrogen bond linking two omega-loops induces the molten globule state at neutral pH in cytochrome *c*. *Biochemistry* **42:** 7604–7610.

Sivakolundu, S.G. and Mabrouk, P.A. 2003. Structure-function relationship of reduced cytochrome *c* probed by complete solution structure determination in 30% acetonitrile/water solution. *J. Biol. Inorg. Chem.* **8:** 527–539.

Skoog, L. and Bjursell, G. 1974. Nuclear and cytoplasmic pools of deoxyribonucleoside triphosphates in Chinese hamster ovary cells. *J. Biol. Chem.* **25:** 6434–6438.

Smulevich, G., Bjerrum, M.J., Gray, H.B., and Spiro, T.G. 1994. Resonance raman spectra and the active site structure of semisynthetic Met80Cys horse heart cytochrome *c*. *Inorg. Chem.* **33:** 4629–4634.

Spolaore, B., Bermejo, R., Zambonin, M., and Fontana, A. 2001. Protein interactions leading to conformational changes monitored by limited proteolysis: Apo form and fragments of horse cytochrome *c*. *Biochemistry* **40:** 9460–9468.

Stellwagen, E. and Cass, R. 1974. Alkaline isomerization of ferricytochrome *c* from *Euglena gracilis*. *Biochem. Biophys. Res. Commun.* **60:** 371–375.

Stewart, J.M., Driedzic, W.R., and Berkelaar, J.A. 1991. Fatty-acid-binding protein facilitates the diffusion of oleate in a model cytosol system. *Biochem. J.* **275:** 569–573.

Stewart, J.M., Blakely, J.A., and Johnson, M.D. 2000. The interaction of ferrocytochrome *c* with long-chain fatty acids and their CoA and carnitine esters. *Biochem. Cell. Biol.* **78:** 675–681.

Svensson, M., Sabharwal, H., Hakansson, A., Mossberg, A.K., Lipniunas, P., Leffler, H., Svanborg, C., and Linse, S. 1999. Molecular characterization of α-lactalbumin folding variants that induce apoptosis in tumor cells. *J. Biol. Chem.* **274:** 6388–6396.

Svensson, M., Mossberg, A.K., Pettersson, J., Linse, S., and Svanborg, C. 2003. Lipids as cofactors in protein folding: Stereo-specific lipid-protein interactions are required to form HAMLET (human α-lactalbumin made lethal to tumor cells). *Protein Sci.* **12:** 2805–2814.

Tuominen, E.K., Zhu, K., Wallace, C.J., Clark-Lewis, I., Craig, D.B., Rytomaa, M., and Kinnunen, P.K. 2001. ATP induces a conformational change in lipid-bound cytochrome *c*. *J. Biol. Chem.* **276:** 19356–19362.

Tuominen, E.K., Wallace, C.J., and Kinnunen, P.K. 2002. Phospholipid-cytochrome *c* interaction: Evidence for the extended lipid anchorage. *J. Biol. Chem.* **277:** 8822–8826.

van der Goot, F.G., Gonzalez-Manas, J.M., Lakey, J.H., and Pattus, F. 1991. A 'molten-globule' membrane-insertion intermediate of the pore-forming domain of colicin A. *Nature* **354:** 408–410.

Zheng, J., Ye, S., Lu, T., Cotton, T.M., and Chumanov, G. 2000. Circular dichroism and resonance Raman comparative studies of wild type cytochrome *c* and F82H mutant. *Biopolymers (Biospectroscopy)* **57:** 77–84.